Beam monitoring and near detector requirements for a Neutrino factory or long-baseline beams

Roumen Tsenov and Rosen Matev

Department of Atomic Physics, St. Kliment Ohridski University of Sofia, 5 James Bourchier Boulevard, Sofia 1164, Bulgaria

E-mail: tsenov@phys.uni-sofia.bg

Abstract. Neutrino Factory is a facility for future precision studies of neutrino oscillations. A so called near detector is essential for reaching the aimed precision of neutrino oscillation analysis. Main task of the near detector is to measure the flux of the neutrino beam. Such brilliant neutrino source like Neutrino Factory provides also opportunity for precision studies of various neutrino interaction processes in the near detector. We discuss design concepts of such a detector. Results of simulations of a high resolution scintillating fiber tracker show that it is capable to measure the neutrino flux through pure leptonic interactions with an uncertainty of less than 1%. A full set-up of the near detector consisting of high granularity vertex detector, high resolution tracker and muon catcher is also presented.

1. Neutrino Factory Near Detector(s) baseline

A future neutrino facility [1] will need near detectors in order to perform oscillation measurements with required sensitivity. It is necessary to have one near detector for each of the straight sections of the storage ring at each of the two polarities, so four near detectors designed to carry out measurements essential to the oscillation-physics programme are required. The near detector tasks include measurement of neutrino flux through the measurement of neutrino-electron scattering; measurement of neutrino beam properties needed for the flux to be extrapolated to the far detector; measurement of charm production cross sections (charm production in far detectors is one of the principal backgrounds to the oscillation signal). In addition, the brilliant Neutrino Factory beam allows for unique neutrino physics non-oscillation studies, such as measurement of cross sections, structure functions, nuclear effects, $\sin^2\theta_W$ *etc.* at neutrino energies in the 0-25 GeV range. The near detector must also be capable of searching for new physics, for example by detecting τ-leptons which are particularly sensitive probes of non-standard interactions at source and at detection. ν_τ detection is also important in a search for sterile neutrino.

Design requirements for the near detector(s) can be formulated as follows: low Z high resolution tracker for flux and cross-section measurement (ν_μ and ν_e); magnetic field for better than in MIND [2] muon momentum measurement; muon catcher and capability for e^+/e^- identification; vertex detector for charmed hadrons and τ-leptons detection (for non-standard interactions and sterile neutrino searches); good resolution on neutrino energy (much better than in the Far Detector) for flux extrapolation.

Current near detector design anticipates three subdetectors (see Fig. 1): high granularity

detector for charm/τ measurement; high resolution tracker for precise measurement of the event close to the vertex and Mini-MIND detector for muon measurement.

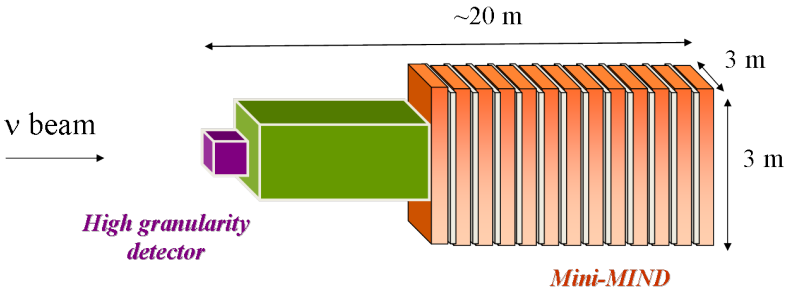

Figure 1. Block diagram design of the Near Detector

2. Measurement of the neutrino flux by neutrino-electron scattering

Neutrino-electron interaction cross sections are straightforwardly calculated in the Standard Model framework. Any small uncertainties could come only from (well measured) Standard Model parameters. Therefore, such processes are suitable for measurement of neutrino beam fluxes, provided that beams are intense enough.

There are two pure leptonic interactions of the Neutrino Factory beam producing a muon in the final state:

$$\nu_\mu + \mathrm{e}^- \to \mu^- + \nu_\mathrm{e} \text{ and } \quad \overline{\nu}_\mathrm{e} + \mathrm{e}^- \to \mu^- + \overline{\nu}_\mu \quad (IMD). \tag{1}$$

The first one is known as inverse muon decay, while the second one produces a muon in the final state through annihilation. The neutrino energy threshold (for electrons at rest) for both processes is 10.9 GeV .

There are four pure leptonic reactions of interest producing energetic electron in the final state:

$$\nu_\mu + \mathrm{e}^- \to \nu_\mu + \mathrm{e}^- \text{and} \quad \overline{\nu}_\mathrm{e} + \mathrm{e}^- \to \overline{\nu}_\mathrm{e} + \mathrm{e}^- \quad (ES^-) \tag{2}$$

$$\nu_\mathrm{e} + \mathrm{e}^- \to \nu_\mathrm{e} + \mathrm{e}^- \text{and} \quad \overline{\nu}_\mu + \mathrm{e}^- \to \overline{\nu}_\mu + \mathrm{e}^- \quad (ES^+). \tag{3}$$

Despite the smallness of the total cross sections for the above processes, a massive detector placed close to the straight section end can provide a sufficient interaction rate - Fig. 2. However, inclusive CC and NC neutrino interactions with nuclei

$$\nu_\ell + N \to \ell + X \text{ and } \quad \nu_\ell + N \to \nu_\ell + X \tag{4}$$

are a few orders of magnitude more intensive. For example, at 15 GeV the muon neutrino CC total cross section is $\sim 1 \times 10^{-37}$ cm^2, compared to $\sim 2 \times 10^{-41}$ cm^2 for inverse muon decay $\nu_\mu \mathrm{e}^- \to \mu^- \nu_\mathrm{e}$. An obvious distinction between purely leptonic processes and processes (4) is the lack of hadronic system X in the former. Thus, the measured recoil energy of the hadronic system can be used as a good criterion for background suppression. Muons from quasi-elastic neutrino-electron scattering have angular distribution peaked at very forward direction. At the Neutrino Factory, the polar angle of these muons does not exceed 5 mrad. The angular spread comes mainly from the intrinsic scattering angle ~ 4 mrad in processes (1), while neutrino beam divergence (and solid angle covered by detector) has little contribution. This kinematic property can be used as another event selection criterion. The polar angle distribution of electrons from neutrino-electron elastic scattering is ten times wider and is not suitable for event selection. On the other hand, the composite variable $\theta_\ell^2 E_\ell$, proportional to Bjorken's $y = 1 - E_l/E_\nu$ in elastic scattering, provides good separation between signal and background for all neutrino-electron scattering processes provided lepton angle and energy are measured with sufficient precision.

Two options for the high-resolution tracker are being considered: *a scintillating fiber tracker* and *a straw tube tracker*.

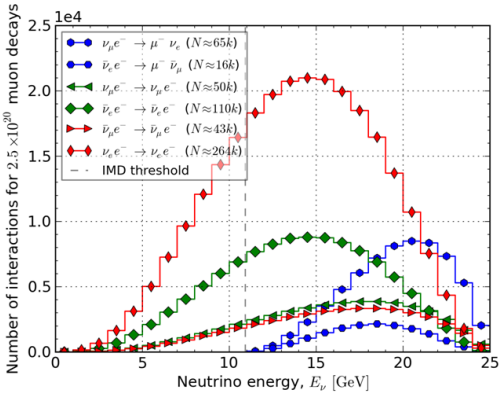

Figure 2. Number of neutrino-electron interactions for 2.5×10^{20} muon decays per muon charge and per straight section– a nominal year of Neutrino Factory operation. Rates are calculated for 2.7 t detector with 1.5 $\times$ 1.5 m^2 frontal cross section and average $Z/A \approx 0.54$. Detector is placed 100 m after the straight section end. Dashed vertical line indicates threshold for the inverse muon decay.

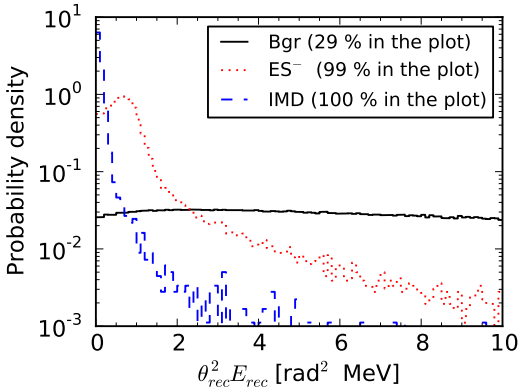

Figure 3. Distributions of reconstructed $\theta^2_\ell E_\ell$ variable for IMD (blue), ES$^-$ (red) and background (black) events in μ^- mode. The fraction of events contained in the plot is indicated in the legend. All distributions are normalized to a unit area.

3. Scintillating fiber tracker

A schematic drawing of a scintillating fiber tracker with an incorporated calorimeter is shown on Fig. 4. The detector consists of 20 square shaped modules placed perpendicular to the beam axis. Each module has a calorimeter section and a tracker section (also called tracker station). Modules are positioned equidistantly forming gaps filled with air. With larger distance between tracker stations, X and Y displacement of hits is increased and thus angular resolution improved. The sides of the air gaps are covered with a layer of plastic scintillating bars. These layers are referred to as *side slabs*. The detector is placed in 0.5 T dipole magnetic field. Each station consists of one layer of fibers with horizontal orientation and another with vertical orientation. Each layer has four planes made of 1 mm round fibers. They form a hexagonal pattern in the layer, thus minimizing dead volume. There are 12 000 fibers per station, thus 240 000 fibers in total. Calorimeter sections consist of plastic scintillating bars perpendicular to the magnetic field and arranged in 5 planes in each section. Bars are co-extruded with a wavelength shifting (WLS) fibers inside and have 10 mm by 30 mm cross-section. Both tracker fibers and WLS fibers in bars are read from both ends by silicon photomultipliers (SiPMs). Overall dimensions of the detector are $\sim$1.5 m $\times$ 1.5 m $\times$ 11 m. The detector mass is $\sim$2.7 t.

3.1. Simulation of the detector response and signal extraction

The neutrino flux at the near detector has been generated by a Monte Carlo simulation of muon decays along the straight section of the Neutrino Factory decay ring [3, 4]. Neutrino interactions in the detector have been simulated by the GENIE package [8]. For the simulation of the detector response to them, the Geant4 software platform [5] was used. Simple algorithms have been developed for vertex and scattered lepton track reconstruction.

The distribution of the difference between the reconstructed and true value of the scattering angle is shown on Fig. 5. The resolution (σ parameter of the fit) is $\sim$0.5 mrad for both muons

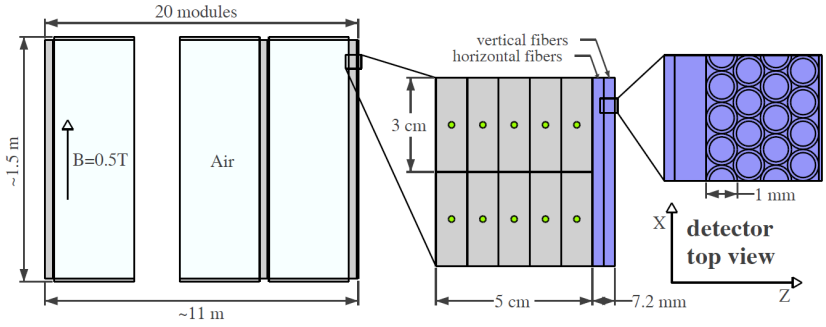

Figure 4. Schematic drawing of the detector.

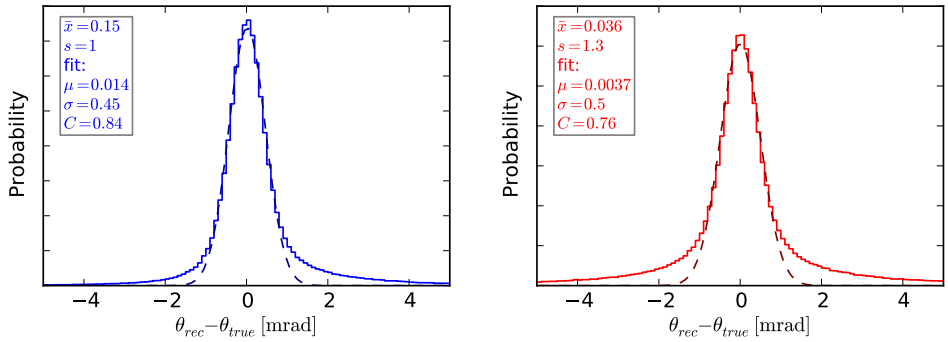

Figure 5. Obtained angular resolution for muons (left) and electrons (right). Gaussian fits are shown with dashed lines.

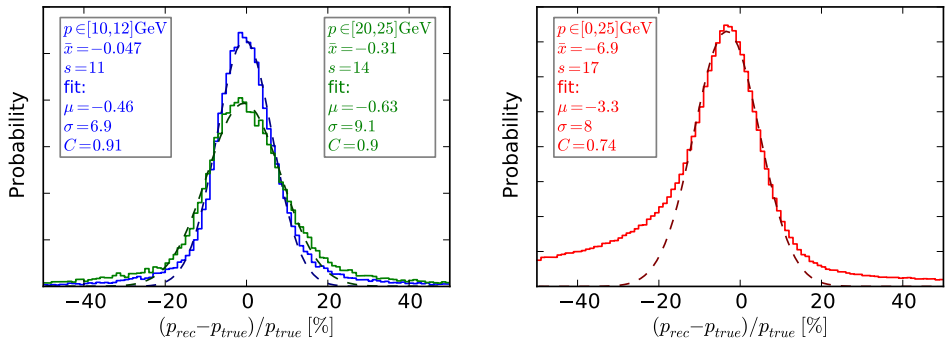

Figure 6. Obtained momentum resolution for muons (left) and electrons (right). Gaussian fits are shown with dashed lines. For muons, distribution is shown for two samples of events: one with true muon momentum in the [10-12] GeV range (blue) and one in the [20-25] GeV range (green).

and electrons. The reconstructed momentum resolution is shown on Fig. 6. For muons it goes up to $\sim$9 % for the highest energy muons. For electrons, the distribution is biased towards the negative values with a heavy negative tail. The reason for this is that they loose momentum due to bremsstrahlung and ionization. If energy loss is taken into account, for instance with Kalman filter fitting [6], bias can be reduced.

Both IMD and ES events have a property of low (consistent with single particle) energy

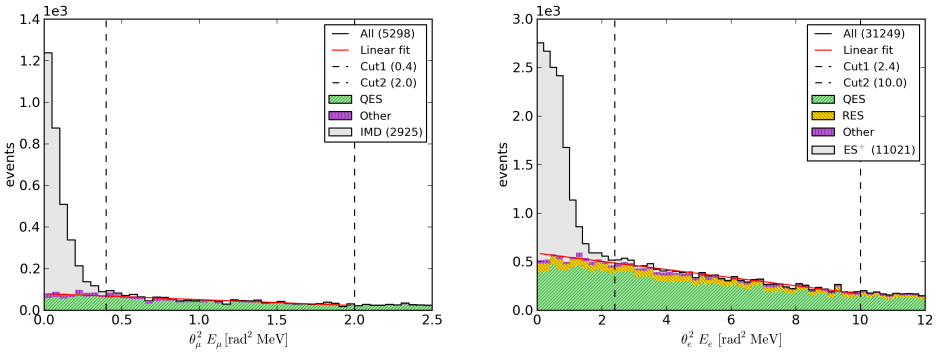

Figure 7. Distributions over $\theta_\mu^2 E_\mu$ for the IMD sample (left) and for the ES$^+$ sample (right). The leptonic events histogram is filled with solid gray, the hadronic events histogram is hatched and the total spectrum is in black. The two cuts bounding the fit interval are drawn with dashed line. The red line indicates the background extrapolation.

deposition near the vertex. To exploit that, a cut on energy deposit around the vertex is imposed. Some other kinematic and calorimetric cuts have also been applied in order to get a sample enriched with signal events. As a result, the signal-to-background ratio has been increased from $\sim 10^{-4}$ to $\sim$30-50 %. Further on, extrapolations of certain background distributions should be made in order to subtract background from event samples. We have chosen to do background subtraction in terms of the primary lepton (μ or e) kinematic variables – the lepton's scattering angle θ_ℓ and initial momentum p measured in the detector. In the case of IMD signal extraction, the scattering angle θ_ℓ and $\theta_\ell^2 E_\ell$ variable can be used to discriminate signal from background. In the case of ES signal, background is well separated only when one exploits the $\theta_\ell^2 E_\ell$ variable. The distributions of $\theta_\ell^2 E_\ell$ for IMD signal, ES$^-$ signal and background are shown on Fig. 3. The background distribution is nearly flat. This fact allows for its simple parameterization.

Two methods of obtaining the number of signal events are discussed below: *the linear fit method* and *the μ^+-method*.

The linear fit method relies on the nearly flat shape of the respective background distribution. The idea is to estimate the background under the signal peak by linear extrapolation from signal-free region towards the signal one. Examples are shown in Fig. 7. Comparison between the estimated and the true number of signal events is made in Table 1. It is seen that the true values lie within the 95 % confidence intervals of the predictions. The systematic uncertainty, estimated as the difference between the fit result and the true number of signal events is less than 1 %. However, to give conclusive estimation of the systematic error, one should investigate if and how various parameters of simulation and selections influence the background shape.

IMD interactions are present only in the μ^- decay mode. The idea of the μ^+-method is to estimate the background under the IMD signal peak exploiting the distribution of positive muons detected in ($\overline{\nu}_\mu$, ν_e)-beam [7]. In the near detector, an event sample from the ($\overline{\nu}_\mu$, ν_e)-beam events is selected with the same selection cuts as the IMD sample. The $\theta_\mu^2 E_\mu$ histogram for μ^+ is normalized to the $\theta_\mu^2 E_\mu$ histogram for μ^-. An interval outside the IMD signal peak and with approximately constant ratio of μ^-- and μ^+-events is defined and the normalization factor is calculated within this interval. The μ^- histogram and the normalized μ^+ histogram are shown in Fig. 8 (left). Subtraction is made using the normalized μ^+ histogram.

Table 1 demonstrates that the number of neutrino-electron scattering events can be measured exploiting the $\theta_\ell^2 E_\ell$ distribution with a good precision. A direct comparison between the

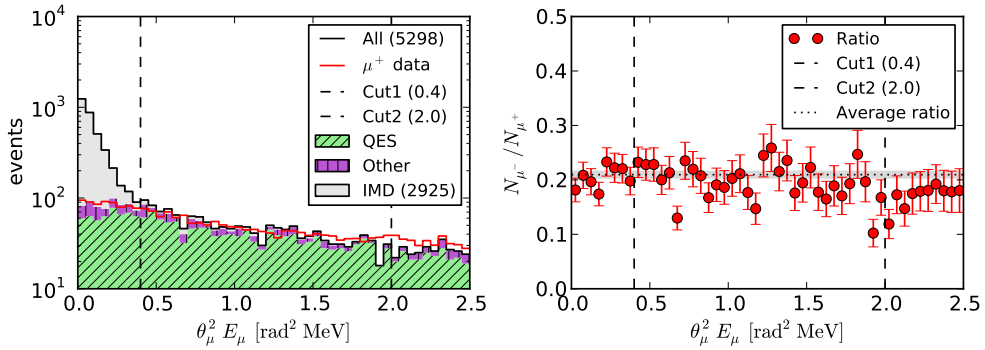

Figure 8. *Left:* distributions over $\theta_\mu^2 E_\mu$ for the IMD sample. The leptonic events histogram is filled with solid gray, the hadronic events histogram is hatched and the total spectrum is in black. The two cuts bounding the normalization interval are drawn with dashed line. The red line indicates the normalized μ^+ histogram. *Right:* ratio of the μ^- histogram and the μ^+ histogram over $\theta_\mu^2 E_\mu$. Horizontal dotted line indicates the (constant) normalization factor.

Table 1. Estimated number of signal events for the three event samples. The result in the last row was obtained using the μ^+ background subtraction method, while the other three results were obtained using linear fit background subtraction method. Statistics correspond to 2.3×10^{19} μ^- decays and 2.3×10^{19} μ^+ decays, which is approximately a tenth of the nominal year.

Event sample	Selection eff.	Overall eff.	Purity	All events	Signal events	Signal events from fit
IMD	86 %	46 %	81 %	3520	2850	2926 ± 59
ES$^-$	70 %	32 %	61 %	7355	4491	4479 ± 86
ES$^+$	83 %	37 %	63 %	16964	10607	10512 ± 131
IMD	86 %	46 %	81 %	3520	2850	2831 ± 61

measured and true number of signal events shows a deviation of no more than 1 %. It is worth noting that the MC truth was not used in reconstruction and signal extraction. Thus, with the presented design of the tracker we can achieve 1% uncertainty on the flux normalisation by exploring IMD and/or ES scattering.

4. High resolution straw tube tracker

Another option for the near detector is a high resolution straw tube tracker inspired by the HiResMν detector [9] being considered for the LBNE project at Fermilab as a near detector.

Building upon the NOMAD experience [11], this low-density tracking detector will have a fiducial mass of 7.4 tons as an active neutrino target, similar to the ATLAS Transition Radiation Tracker [12] and the COMPASS detector [13]. The tracker will be composed of straw tubes with 1 cm diameter, in the vertical (y) and horizontal (x) direction. In front of each module a plastic radiator made of many thin foils allows the identification of electrons through their transition radiation. The nominal fiducial volume is: $350 \times 350 \times 600$ cm^3, corresponding to 7.4 tons of mass with an overall density $\rho < 0.1$ g/cm^3. The straw-tube tracker will be surrounded by

an electromagnetic calorimeter (sampling Pb/scintillator) covering the forward and side regions. Both sub-detectors will be installed inside a dipole magnet providing a magnetic field of ~ 0.4 T.

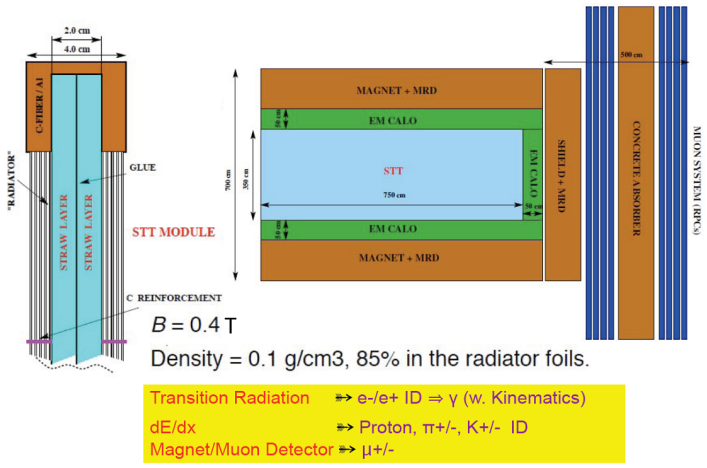

Figure 9. Sketch of the proposed HiRes detector showing the inner straw tube tracker (STT), the electromagnetic calorimeter (EM CALO) and the magnet with the muon range detector (MRD). Also shown is one module of the proposed straw tube tracker (STT). Two planes of straw tubes are glued together and held by an aluminium frame.

The detector will provide full reconstruction of charged particles and γs; identification of electrons, pions, kaons, and protons from dE/dx; electron (positron) identification from transition radiation ($\gamma > 1000$); full reconstruction and identification of recoil protons down to momenta of 250 MeV; reconstruction of electrons down to momenta of 80 MeV from curvature in the B-field.

Detailed simulations of this detector have been carried out in the context of the LBNE proposals [10]. These simulations are to be adapted to the neutrino spectra at a Neutrino Factory to derive the performance parameters of this detector in this context.

5. Charm and Tau Detector

A near detector at a neutrino factory needs to measure the charm cross-section to validate the size of the charm background in the far detector, since this is the main background to the wrong-sign muon signature. The charm cross-section and branching fractions are poorly known, especially close to threshold. For this reason, it is paramount to make an independent near detector measurement of the charm cross-section and make the error in the charm cross-section negligible in the estimation of the neutrino oscillation background.

Since events with a τ-lepton in the final state have a similar signature to charm events, any detector that can measure charm should be able to measure τ's as well. This is important to explore couplings of Non Standard Interactions (NSI) at source $\epsilon^s_{\tau\mu}$, $\epsilon^s_{\tau e}$ or detection $\epsilon^d_{\tau\mu}$, $\epsilon^s_{\tau e}$ A semiconductor vertex detector for charm and τ-lepton detection could potentially be used for this purpose. The advantage of this type of detector is that it is able to operate at a high event rate and still have very good spatial resolution. This is necessary to distinguish the primary neutrino interaction vertex from the secondary vertex due to the short lived charm hadron or the τ-lepton. The vertex detector could be similar to the NOMAD–STAR detector that was installed upstream of the first drift chamber of the NOMAD neutrino oscillation experiment [11] used to measure the impact parameter and double vertex resolution to determine the charm detection efficiency. The reconstruction of τ-leptons from an impact parameter signature with a dedicated silicon vertex detector was studied in the NAUSICAA proposal [14]. A silicon vertex detector with a B_4C target was proposed as an ideal medium to identify τ-leptons. Standard ν_μ CC interactions have an impact parameter $r.m.s$ of 28 μm, while tau decays have an impact parameter$r.m.s$ of 62 μm. By performing a cut on the impact parameter significance (σ_{IP}/IP) one can separate one prong decays of the tau from the background. For three prong decays of

the tau, a double vertex signature is used to separate signal from background. The total net efficiency of the tau signal in NAUSICAA was found to be 12%.

A silicon strip vertex detector as part of the near detector could have the following dimensions [1]: 18 layers of B_4C (2.49 g/cm^3), 150x150x2 cm^3 each; total mass = 2.02 tonnes, 20 layers of silicon strip or pixel detectors, e.g. 45 m^2 of silicon; about 64 000 channels per layer, 1.28 million channels in total. At the Neutrino Factory in such a detector about 3×10^7 ν_μ CC interactions per year are expected and 10^6 charm events among them. With the efficiency of the tau detection found in NAUSICAA, one could have a sensitivity of $P_{\mu\tau} < 3 \times 10^{-6}$ at 90% C.L. on the $\nu_\mu \to \nu_\tau$ conversion probability.

6. Summary and outlook

A near detector(s) at the Neutrino factory is a valuable tool for neutrino flux measurement and standard and non-standard neutrino interactions. The envisioned set-up consists of high granularity vertex detector followed by high resolution tracker and muon catcher. Silicon vertex detector+SciFi tracker+mini-MIND set-up is most advanced with respect to simulations with Neutrino Factory beam. They show that the neutrino flux can be measured with 1% uncertainty. A second option exists for the tracker – HiResMν. Simulations with a Neutrino Factory beam are needed to confirm its ability to select and measure neutrino-electron scattering.

Further tasks include the simulation of the full set-up in order to estimate systematic errors coming from near-to-far extrapolation (determination of the so-called *migration matrices*); expectation on cross-section measurements and other physics studies, sensitivity to non-standard interactions (τ-lepton production). In a bit more distant future, serious R&D efforts would be needed to validate the technology choices for the vertex detector, high-resolution tracker, *etc.*

References

[1] Choubey S *et al.* 2011 Interim Design Report of the International Design Study for the Neutrino Factory *Preprint hep-ex/1112.2853*

[2] Laing A Ph.D. Thesis (University of Glasgow: 2010) `http://theses.gla.ac.uk/2216/`

[3] Karadzhov Y 2010 *AIP Conf. Proc.* **1222** 467–70

[4] Karadzhov Y and Tsenov R 2010 *Annual of University of Sofia, Faculty of Physics* **103** `http://www.phys.uni-sofia.bg/annual/arch/103/full/GSU-Fizika-103-06_full.pdf`

[5] Agostinelli S *et al.* (GEANT4 Collaboration) 2003 *Nucl. Instrum. and Methods* A **506** 250–303; Amako K, Apostolakis J, Araujo H and Dubois P *et al.* 2006 *IEEE Trans. Nucl. Sci.* **53** 270

[6] Kalman R E 1960 *Transactions of the ASME–Journal of Basic Engineering*, Series D, **82** 35–45

[7] Geiregat D*et al.* (CHARM-II Collaboration) 1990 *Phys. Lett.* B **247** 131–6; Vilain P *et al.* (CHARM-II Collaboration) 1995 *Phys. Lett.* B **364** 121–6

[8] 2010 Andreopoulos C *et al.*, *Nucl. Instrum. and Methods* A **614** 87–104 (*Preprint hep-ph/0905.2517*)

[9] Mishra S R, Petti R and Rosenfeld C 2008 *PoS*, **NUFACT08** 069 (*Preprint hep-ex/0812.4527*)

[10] *Long Baseline Neutrino Experiment*, `http://lbne.fnal.gov/` (2010).

[11] Altegoer J *et al.* (NOMAD collaboration) 1998 *Nucl. Instrum. and Methods* A **404** 96–128

[12] Akesson T *et al.* (ATLAS TRT collaboration) 2004 *Nucl. Instrum. and Methods*, A **522** 131–45 and 50–3; Abat E *et al.* (ATLAS TRT collaboration) 2008 *JINST*, **3** P02013.

[13] Bychkov V N *et al.* 2002 *Part. Nucl. Lett.* **111** 64–73

[14] Gomez-Cadenas J J, Hernando J A and Bueno A 1996 *Nucl. Instrum. and Methods* A **A378** 196–220